Gas phase ion chemistry and ab initio theoretical study of phosphine. I

Paola Antoniotti, Lorenza Operti, Roberto Rabezzana, Maurizio Splendore, Glauco Tonachini, and Gian Angelo Vaglio

Citation: The Journal of Chemical Physics **107**, 1491 (1997); doi: 10.1063/1.474502
View online: http://dx.doi.org/10.1063/1.474502
View Table of Contents: http://scitation.aip.org/content/aip/journal/jcp/107/5?ver=pdfcov
Published by the AIP Publishing

Gas phase ion chemistry and *ab initio* theoretical study of phosphine. I

Paola Antoniotti, Lorenza Operti,[a] Roberto Rabezzana, Maurizio Splendore, Glauco Tonachini,[a] and Gian Angelo Vaglio
Dipartimento di Chimica Generale ed Organica Applicata, Università degli Studi di Torino, Corso Massimo d'Azeglio 48, 10125 Torino, Italy

(Received 10 February 1997; accepted 23 April 1997)

Gas phase ion processes of phosphine have been studied by theoretical calculations and experimental techniques. *Ab initio* quantum chemical calculations have been performed on the ion/molecule reactions starting from P^+ in PH_3, as they have been observed by ion trapping. P^+ gives $P_2H_n^+$ $(n=1,2)$ product ions with loss of H_2 or H in different pathways and also reacts in charge-exchange processes to form PH_3^+. The energies of transition structures, reaction intermediates, and final products, as well as their geometrical structures have been determined by theoretical methods. The initial step is formation of a triplet $P_2H_3^+$ adduct of C_{3v} symmetry $(P{-}PH_3^+)$. A hydrogen atom can either be directly lost from the tetracoordinated phosphorus, or first undergo a shift to the other P atom $(HP^+{-}PH_2)$, followed by P–H bond dissociation. Dissociation of H_2 from $P_2H_3^+$ can also occur from both the initial $P{-}PH_3^+$ and $HP^+{-}PH_2$ species yielding PPH^+. The heats of formation of the $P_2H_n^+$ ionic species have also been computed and compared with experimental data reported in the literature. © *1997 American Institute of Physics.* [S0021-9606(97)00529-1]

I. INTRODUCTION

Amorphous materials consisting of hydrogenated elements of group 14 of the Periodic Table doped with phosphorus are promising in electronic and optoelectronic applications, because of the marked improvement of their electric properties.[1–5] Possible techniques to prepare these materials are low pressure,[2,6] rapid thermal,[3] ultrahigh vacuum,[4] or radiolytically activated chemical vapor deposition[7–9] (CVD), starting from gaseous mixtures containing volatile hydrides of germanium or silicon with phosphine. The relative abundance of each element in the final product depends on the partial pressure of the respective hydride in the gas mixture, but not in a direct or predictable way. In order to find the effect of the concentration of a gaseous reactant on its abundance in the solid, it is of fundamental importance to know in detail the gas phase behavior of each of the reacting molecules.

In previous studies, the interpretation of the mechanisms involved in x-ray assisted CVD and of gas phase behavior of volatile systems has been successfully obtained by mass spectrometric methods.[10–15] Moreover, the combination of experimental and theoretical investigations is becoming a usual and useful approach to the study of gas phase ion chemistry, as complementary informations are obtained.[14–18] In fact, the mechanisms and energetics of the reactions observed experimentally, together with the structures of the ion products, can be investigated by *ab initio* calculations.[15–19]

In this paper we report results of *ab initio* quantum chemical calculations on the reaction pathways starting from P^+ in phosphine, as they have been determined by ion trap mass spectrometry. Theoretical calculations have been used to determine the geometries and energies of transition structures, reaction intermediates and final products of reaction pathways starting from the P^+ primary ion. Moreover, the rate constants for the first nucleation reactions have been experimentally measured and compared with the rate constants calculated according to the average dipole orientation (ADO) theory.[20]

Investigations on phosphine alone or in mixtures have been previously performed by different mass spectrometric methods[6,10,15,21] concerning some of the reactions observed in this study. Heats of formation and bond energies of both neutral and ionic P–H compounds, together with ionization potentials of neutrals, have been determined by theoretical calculations.[16]

II. EXPERIMENTAL PROCEDURES

Phosphine was obtained commercially in high purity. It was introduced into a flask, containing anhydrous sodium sulfate as drier, which was connected to one line of the gas inlet system of the instrument. Helium was supplied at an extra-high purity degree and used without further purification. All experiments were run on an ITMS 70 Finnigan MAT mass spectrometer. A Bayard–Alpert ionization gauge was used to measure pressure. The read pressures were corrected for the relative sensitivity of the ion gauge with respect to phosphine[22] and for a calibration factor, calculated as reported previously,[10] to obtain the real pressure in the trap. Helium buffer gas was admitted to the trap at a pressure of about 4×10^{-4} Torr. The temperature of the trap was maintained at 333 K, at which other related systems have been studied. In all experiments, ions were detected in the 10–200 u mass range. In order to prevent side reactions with water background, the manifold and the lines for introduction of phosphine and helium were frequently baked-up. The scan modes used in these experiments, both to study the

[a]Authors to whom correspondence should be addressed.

overall ion reactivity as a function of time and to determine reaction mechanisms and rate constants, have been described in detail previously, as well as the procedures for calculations.[10]

In the kinetic experiments the isolation of ions at a specific m/z value was obtained by using dc voltages and by resonance ejection, as described previously.[10] In the latter isolation method no field is directly applied on the selected ionic species and, therefore, the ions should have a lower excitation energy. The rate constants obtained by using these two different isolation procedures are very similar. This is in agreement with the hypothesis that the reactant ions undergo a number of collisions sufficient to eliminate most of their excitation energy. The single exponential decays observed in the kinetic experiments are consistent with this hypothesis.

In all experiments ionization was obtained by electron impact for times in the range 1–10 ms. In experiments without selective storage of ions, ionization is followed by a reaction time, which ranges from 0 to 500 ms, without application of any potential to the trap. Acquisition of ion signal closes the experiment. When isolation of an ion species is performed, after the ionization event, a reaction time follows in order to maximize the abundances of the ions under examination. Isolation of the selected ions, storage in the trap for convenient reaction times and acquisition are the successive events.

III. THEORETICAL METHODS

The study of the H atom rearrangement and dissociation processes, as well as H_2 dissociation, in the $P_2H_3^+$ triplet molecule was performed by determining, on the reaction energy hypersurface, the critical points relevant to stable and transition structures. This was accomplished by way of complete gradient optimization[23] of the geometrical parameters at the complete active space (CAS) MCSCF and UMP2 levels of theory,[24,25] using the polarized split-valence shell 6-31G(d) basis sets.[26] The UMP2/6-31G(d) geometries were characterized as energy minima or first order saddle points (transition structures) by diagonalization of the analytically computed Hessian (vibrational frequencies calculations).[27] In one case (a bridged H-shift transition structure) the 6-31G(d,p) basis set,[26] containing also p polarization functions on the hydrogens, was used; however, the effect of these additional functions on the optimized geometry was found to be modest. In the figures of the following section the reported interatomic distances are in angströms and angles in degrees (HPPH dihedral angles in parentheses). The UMP2/6-31G(d) geometries were used to recompute the relative energies by quadratic configuration interaction calculations at the QCISD(T) level,[28] in conjunction with the more extended basis set 6-311G($2d,2p$).[26] The basis set superposition error[29] (BSSE) was estimated at both MP2/6-31G(d) and QCISD(T)/6-311G($2d,2p$) levels, in relation with the first process, in which the $P_2H_3^+$ adduct is formed from P^+ and PH_3, and also with the charge-exchange process, yielding the P atom and PH_3^+ ions. Zero-point vibrational energies[27,29] were computed at the MP2/6-31G(d) level. The GAUSSIAN94 system of programs[30] was used throughout, on IBM RISC/6000 computers at the Dipartimento di Chimica Generale ed Organica Applicata.

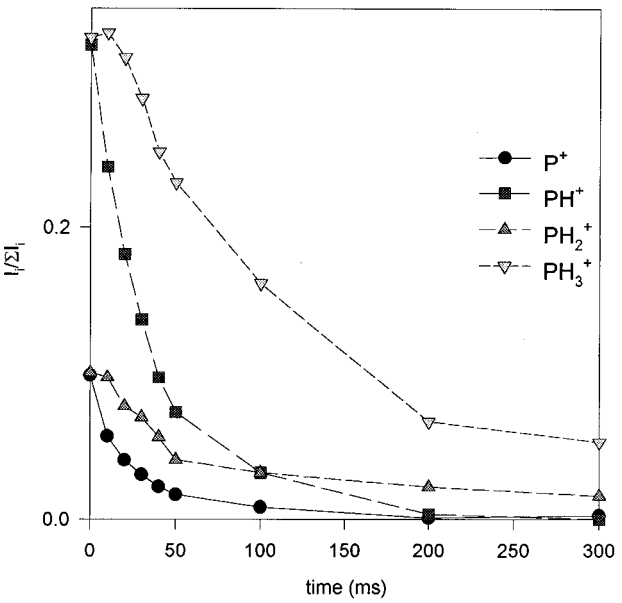

FIG. 1. Variations in ion abundances with time for P^+, PH^+, PH_2^+, and PH_3^+ primary ions in PH_3 (6.8×10^{-7} Torr).

IV. RESULTS AND DISCUSSION

A. Mass Spectrometric Determinations

Figures 1 and 2 report the variation of the relative abundances of all the primary ions (Fig. 1) and of the most sig-

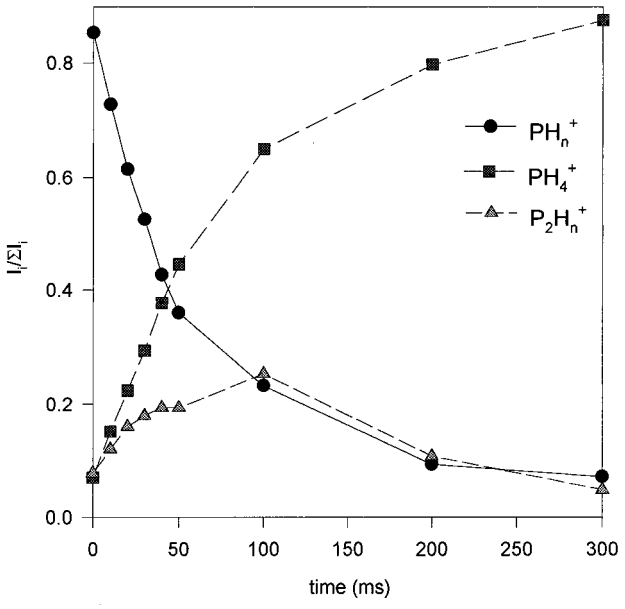

FIG. 2. Variations in ion abundances with time for PH_n^+ ($n=0-3$), PH_4^+, and $P_2H_n^+$ ($n=0-3$) ion families in PH_3 (6.8×10^{-7} Torr).

nificant ionic families (Fig. 2) in the ion trap mass spectra of PH_3 at a pressure of 6.8×10^{-7} Torr at reaction times from 0 to 300 ms.

At zero reaction time, the primary ions transport 85.4% of the total ion current, the most abundant ions being PH^+ and PH_3^+, which lead an odd number of hydrogen atoms. As the reaction time increases, the abundances of the primary ions decrease, while the abundance of the product ions, PH_4^+ and $P_2H_n^+$ $(n=0-3)$, quickly grows. However, the secondary ions follow different trends as the abundance of the $P_2H_n^+$ $(n=0-3)$ ionic family increases up to 100 ms of reaction and then decreases while the abundance of PH_4^+ continuously increases up to 300 ms reaction time (88.0% of the total ion current).

Scheme 1 shows the reaction pathways observed starting

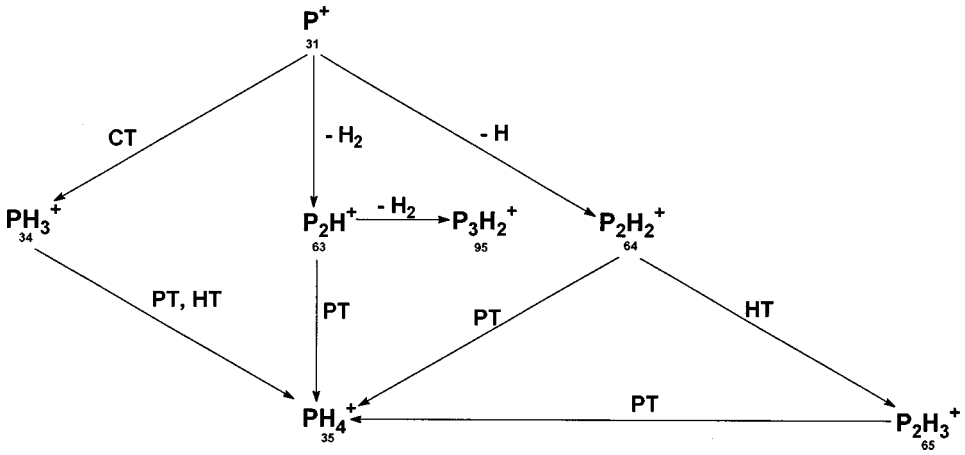

from the primary ion P^+. The most common pathways shown in this scheme are loss of $H_2(-H_2)$ and proton transfer (PT). Also charge transfer (CT) is observed, as well as the loss of H (–H) and hydrogen atom transfer (HT) process. The scheme was built by isolating and storing the primary ions for reaction times up to 500 ms, and by detecting all ion species produced during that delay time. Every product ion was in turn isolated and reacted for variable times, and its ionic products were detected. This procedure was repeated until product ions were abundant enough to be isolated. The thermochemical data[21,31] relative to the addition of PH and elimination of H_2, as reported in the following pathway:

$$P^+ + PH_3 \rightarrow P_2H^+ + H_2 \quad (1)$$

indicate that this process is exothermic. In fact, loss of a hydrogen molecule is very common in gas phase ion chemistry and it has been observed in the growth processes of $Si_nH_{n+2}^+$ and $Ge_mH_{m+2}^+$ clusters from SiH_4 and GeH_4, respectively.[13,32,10]

Another pathway leads to the loss of a hydrogen atom. This reaction, even if thermodynamically favored, is less exothermic than the preceding one.

P^+ reacts with PH_3 in a charge-exchange process to give PH_3^+, which, in turn, transfers a proton to phosphine to form PH_4^+, as the only product, which is unreactive in the reaction time here examined. On the basis of thermodynamic data, this path is exothermic as well.

An ionic product containing three atoms of phosphorus, $P_3H_2^+$, was detected, which originates from P_2H^+ reacting with phosphine through the loss of one molecule of hydrogen.

Table I reports the rate constants determined in this study for the reactions of P^+ and its product ions with PH_3. The collisional rate constants calculated according to the ADO theory[20] and the efficiencies of reactions are also shown in this table. The reactions show very high efficiencies, which are the ratios between the experimental and calculated rate constants. These efficiencies are slightly higher than a unit for the primary ions P^+ and PH_3^+, (probably due to experimental error) and slightly lower than unit for the secondary ionic species, P_2H^+ and $P_2H_2^+$, meaning that they all react at collisional rates. Moreover, the condensation pro-

TABLE I. Rate constants for reactions of P^+ and its product ions in self-condensation of PH_3.[a]

Reaction	k_{exp}	Σk_{exp}	k_{ADO}^{b}	Efficiency[c]
$P^+ + PH_3 \rightarrow PH_3^+ + P$	3.9			
$P^+ + PH_3 \rightarrow P_2H^+ + H_2$	8.2			
$P^+ + PH_3 \rightarrow P_2H_2^+ + H$	0.7	12.8	11.56	1.11
$PH_3^+ + PH_3 \rightarrow PH_4^+ + PH_2$	12.4	12.4	11.28	1.10
$P_2H^+ + PH_3 \rightarrow PH_4^+ + P_2$	7.9			
$P_2H^+ + PH_3 \rightarrow P_3H_2^+ + H_2$	0.5	8.4	9.90	0.85
$P_2H_2^+ + PH_3 \rightarrow PH_4^+ + P_2H$	8.0			
$P_2H_2^+ + PH_3 \rightarrow P_2H_3^+ + PH_2$	0.8	8.8	9.87	0.89

[a]Rate constants are expressed as 10^{-10} cm^3 molecule^{-1} s^{-1}; experiments were run at 333 K; uncertainty is within 20%.
[b]Rate constants have been calculated according to the ADO theory (Ref. 20) calculating polarizability and taking the dipole moment from Ref. 29(a).
[c]Efficiency has been calculated as the ratio k_{exp}/k_{ADO}.

cess to give P_2H^+ and eliminate H_2 has a high rate constant, while formation of $P_2H_2^+$ with loss of a hydrogen atom occurs with a rate constant which is lower then the previous one by an order of magnitude. When reactions of the secondary ions are considered, the fastest process leads to the formation of PH_4^+ and the condensation reaction yielding $P_3H_2^+$ occurs at a very low rate. The rate constants for self-condensation reactions of P^+ and PH_3^+ have been determined previously[21] and they are in good agreement with our results.

B. Theoretical Study of the Reactions

In *ab initio* theoretical calculations the following chemical processes were considered: (1) the formation of the initial triplet $P–PH_3^+$ adduct from P^+ and PH_3; (2) the charge-exchange process which produces the new P atom and PH_3^+ ion; (3) hydrogen atom or hydrogen molecule dissociations from $P–PH_3^+$; (4) H migration from one phosphorus atom to the other, giving $HP^+–PH_2$; and (5) the ensuing hydrogen atom or hydrogen molecule dissociations. The first part of the study consisted in determining the critical point geometries at the complete active space (CAS) MCSCF/ 6-31G(d) level of theory, using an active space defined by eight electrons in eight orbitals.[33] This first phase was particularly aimed to examine, right from the onset, the nature of the wave function in the different processes, and allowed to settle to what extent a single reference wave function had to be expected to provide a qualitatively acceptable description of the potential energy hypersurface. In a second phase, the critical point geometries were redetermined by perturbative MP2 optimizations, in conjunction with the same basis sets used in the previous calculations. The results of these two sets of calculations will be presented in the following for each reaction pathway.

1. Formation of triplet $P–PH_3^+$

The initial step is the reaction of a triplet P^+ ion with phosphine, which brings about the formation of a triplet $P–PH_3^+$ adduct of C_{3v} symmetry (Fig. 3, 1a). The P–P bond length, 2.226 Å, is close to that found for neutral P_2H_4 and has basically the nature of a single P–P bond.[34] The MCSCF wave function for this species has one dominant configuration (Table II), corresponding to a single occupancy of two orbitals which are essentially localized on that phosphorus atom which carries no hydrogens (i.e., two p orbitals orthogonal to the P–P bond). The UMP2 optimization produced quite a similar geometry (for instance, the P–P bond length is 2.221 Å). This kind of computation is based on a previous UHF calculation, which can be affected by a contamination by spin multiplicities higher than the triplet; however, the total spin eigenvalue $\langle S^2 \rangle$ appears in this case to be sufficiently close to 2 (Table III), and consequently the contamination extent is moderate. Projected MP2 energy values are as well reported in Table III.[35]

The estimate of the energy gain achieved in going from the two reactants to the adduct is important in that all the subsequent processes are certainly possible if the relevant energy barriers are lower than the amount of kinetic energy

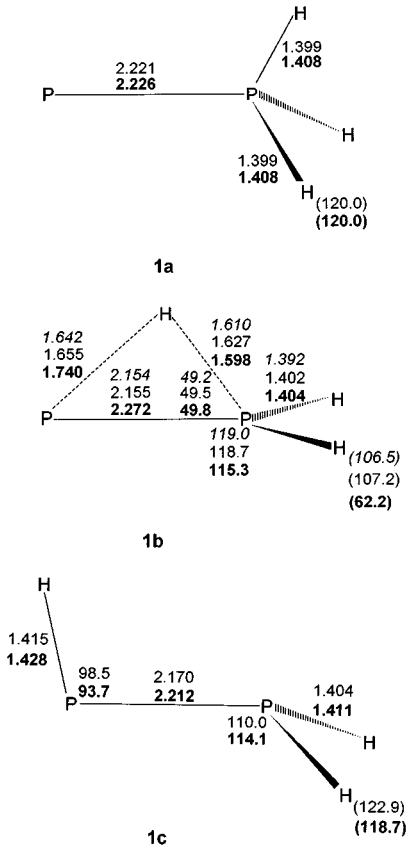

FIG. 3. H migration from $P–PH_3^+$ to $HP^+–PH_2$; (1a) adduct of C_{3v} symmetry; (1b) transition structure for the [1,2] shift; (1c) rearranged ion. Bond distances are in angström, and bond angles in degrees. CAS-MCSCF/6-31G(d) (bold), MP2/6-31G(d), and MP2/6-31G(d,p) (italic) values are shown.

acquired by the system in the first step. In this respect, the MP2/6–31G(d) estimate, -82.9 kcal mol^{-1}, and the QCISD(T)/6–311G($2d$,$2p$) one, -80.9 kcal mol^{-1} (Tables III and IV), can be expected to suffer from some basis set superposition error. An assessment of the magnitude of this

TABLE II. Total and relative energies (hartree and kcal mol^{-1}) for the reaction of $P^+ + PH_3$.

	Structure	CASSCF/6-31G(d)	ΔE	Largest Cl coefficient[a]
1a	$P_2H_3^+$	$-682.932\,438$	0.0	0.984
1b	$P(H)PH_2^+$ (H migration TS)	$-682.848\,978$	52.4	0.968
1c	$HP_2H_2^+$	$-682.898\,008$	21.6	0.982
2a	$P_2(H)H_2^+$ (H elimination TS)	$-682.825\,940$	66.8	0.933
	$P_2(H)H_2^+$ (complex)	$-682.826\,105$	66.7	0.938
2b	$(H)P_2H_2^+$ (H elimination TS)	$-682.822\,745$	68.8	0.932
2c	$HP_2H(H)^+$ (H elimination TS)	$-682.800\,164$	83.0	0.938
2d	$P_2H_2^+ + H$	$-682.825\,763$	66.9	0.939
2e	$HP_2H^+ + H$	$-682.801\,976$	81.9	0.936
3a	$P_2H(H_2)^+$ (H_2 elimination TS)	$-682.824\,400$	67.8	0.977
	$P_2H(H_2)^+$ (complex)	$-682.837\,008$	59.9	0.882
3b	$HP_2(H_2)^+$ (H_2 elimination TS)	$-682.796\,492$	85.3	0.974
3c	$P_2H^+ + H_2$	$-682.836\,638$	60.1	0.882

[a]Largest Cl coefficients of the ground state of the MCSCF wave function.

TABLE III. Total and relative energies (hartree and kcal mol^{-1}) for the reaction $P^+ + PH_3$.

		$\langle S^2\rangle$[a]	UMP2	ΔE	PMP2	ΔE	ZPE[b]	ΔZPE
	$P^+ + PH_3$		−682.945 242	0.0	−682.946 214	0.0		
			−682.952 030[c]	0.0[c]	−682.953 228[c]	0.0[c]	15.7	−2.5
1a	$P_2H_3^+$	2.0215	−683.077 346	−82.9	−683.079 245	−83.5	18.2	0.0
				−78.6[c]		−79.1[c]		
1b	$P(H)PH_2^+$ (H migration TS)	2.0803	−683.995 984	−31.8	−683.001 149	−34.5	14.5	−3.7
1c	$HP_2H_2^+$	2.0314	−683.046 773	−63.7	−683.046 773	−63.1	16.5	−1.7
2b	$(H)P_2H_2^+$ (H elimination TS)	2.0914	−682.969 387	−15.2	−682.974 116	−17.5	13.4	−4.8
2c	$HP_2H(H)^+$ (H elimination TS)	2.3192	−682.948 008	−1.7	−682.955 799	−6.0	12.1	−6.1
	$(H)P_2H_2^+$ (complex)	2.0204	−682.973 606	−17.8	−682.975 254	−18.2	12.4	−5.8
2d	$P_2H_2^+ + H$	0.7996	−682.971 965	−16.8	−682.974 750	−17.9	11.3	−6.9
2e	$HP_2H^+ + H$	0.7939	−682.964 047	−11.8	−682.968 219	−13.8	14.4	−3.8
3a	$P_2H(H_2)^+$ (H_2 elimination TS)	2.0761	−682.974 729	−18.5	−682.978 036	−20.0	14.1	−4.1
3b	$HP_2(H_2)^+$ (H_2 elimination TS)	2.0353	−682.960 222	−9.4	−682.963 100	−10.6	13.5	−4.7
3c	$P_2H^+ + H_2$	2.0154	−682.973 520	−17.7	−682.975 259	−18.2	11.7	−6.5
	$P + PH_3^+$		−682.981 213	−22.6	−682.982 214	−22.6	15.7	−2.5
			−682.986 974[c]	−21.9[c]	−682.988 002[c]	−21.8[c]		

[a]Eigenvalues of spin operator at the UHF/6-31G(d) level of theory.
[b]Zero-point energies (kcal mol^{-1}) at the MP2/6-31G(d) level of theory.
[c]With counterpoise correction of the basis set superposition error.

error provides the values of 4.3 (MP2) and 2.5 (QCI) kcal mol^{-1}. Thus, the limiting energy value (for ideal collisions tending to zero kinetic energy) is set to 78.6 kcal mol^{-1} (for the MP2 barriers to be presently discussed), or 78.4 kcal mol^{-1} (for the QCI estimate of the same barriers).

2. Charge exchange process

The energy associated with Eq. (2),

$$P^+ + PH_3 \rightarrow P + PH_3^+ \quad (2)$$

(Tables III and IV) can also be corrected for the basis set superposition error. This gives an energy difference of −21.9 (UMP2) and −15.2 (QCI) kcal mol^{-1}. The P and PH_3^+ moieties are thus estimated to lie 60.3 (UMP2) or 65.7 (QCI) kcal mol^{-1} above the initial adduct 1a.

TABLE IV. Total and relative energies (hartrees and kcal mol^{-1}) for the reaction of $P^+ + PH_3$.

	Structure	QCISD(T)/6-311G(2d,2p)[a]	ΔE
	$P^+ + PH_3$	−683.081 521	0.0
		−683.085 444[b]	0.0[b]
1a	$P_2H_3^+$	−683.210 445	−80.9
			−78.4[b]
1b	$P(H)PH_2^+$ (H migration TS)	−683.140 410	−37.0
1c	$HP_2H_2^+$	−683.182 530	−63.4
2d	$P_2H_2^+ + H$	−683.097 071	−9.8
2e	$HP_2H^+ + H$	−683.085 613	−2.6
3c	$P_2H^+ + H_2$	−683.108 975	−17.2
	$P + PH_3^+$	−683.105 874	−15.3
		−683.109 680[b]	−15.2[b]

[a]Calculated using UMP2/6-31G(d) optimized geometries.
[b]With counterpoise correction of the basis set superposition error.

3. H atom migration from $P-PH_3^+$ to HP^+-PH_2 (pathway 1)

A hydrogen atom can either be directly lost from the tetracoordinated phosphorus in 1a, or first undergo a [1,2] shift to the other P atom, followed by P–H bond dissociation. At both CAS-MCSCF and MP2 levels of theory the rearrangement does not require to overcome a prohibitive (in this context) energy barrier; slightly more than 50 kcal mol^{-1} are estimated to separate the transition structure for the [1,2] shift (Fig. 3, 1b) from the initial adduct (Tables II and III). A redetermination of this structure at the MP2 level, using the 6-31G(d,p) basis set, which is polarized in a more balanced way, shows that adding p functions on the hydrogens has a very limited effect on the geometry. Consequently, the 6-31G(d) basis set was henceforth used. The rearranged ion, HP^+-PH_2 (Fig. 3, 1c), lies ~20 kcal mol^{-1} above 1a.

4. H atom dissociations from $P-PH_3^+$ and HP^+-PH_2 (pathways 2)

Investigation of the possible bond cleavages at the CAS-MCSCF level of theory[33] provided the basic information that a single configuration definitely dominates all along the reaction pathways (Table II). Two different P–H bond cleavage processes pass through transition structures (Fig. 4, 2a, 2b) of similar energy, lower than 70 kcal mol^{-1}. These pathways consequently appear to be viable to the reacting system. In contrast, a third transition structure (Fig. 4, 2c) is associated to a barrier ~10 kcal mol^{-1} higher, and appears to be less promising. While the first two pathways converge onto the same dissociation limit, $H + P^+ = PH_2$ (Fig. 4, 2d), the third one is related to the $[HP{=}PH]^+$ (Fig. 4, 2e) and H fragments. Structure 2a was optimized at the CAS-MCSCF level only; although unable to optimize a MP2 transition structure, we have defined an approximate dissociation path-

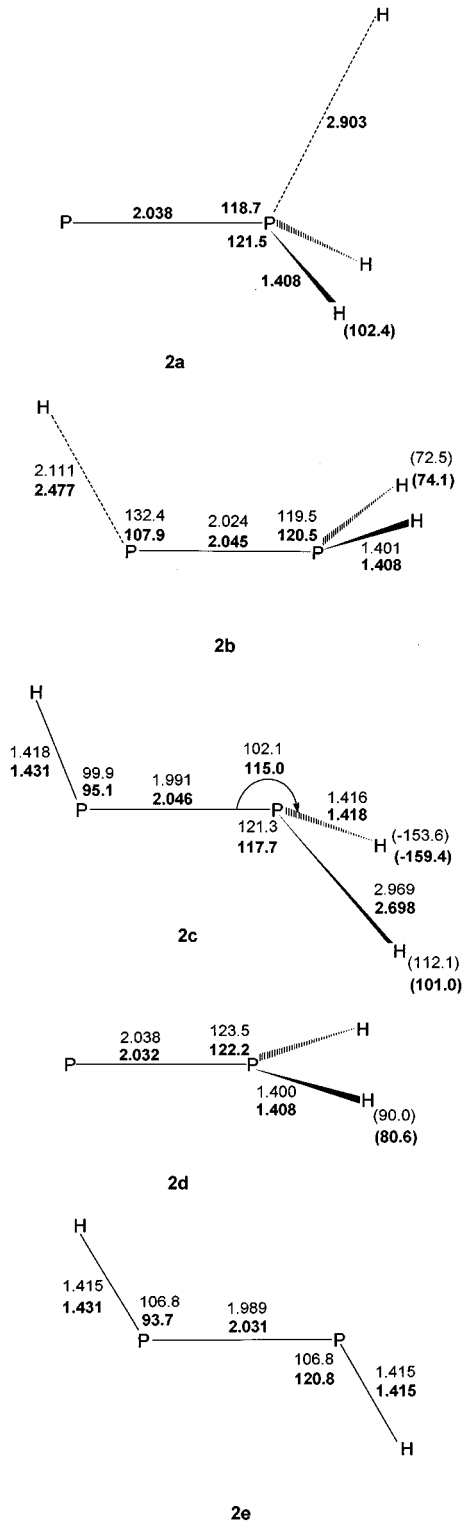

FIG. 4. H atom dissociation from $P–PH_3^+$ and $HP^+–PH_2$; (2a) transition structure for the dissociation from 1a; (2b) first transition structure for the dissociation from 1c; (2c) second transition structure for the dissociation from 1c; (2d) product of the first two pathways, 2a and 2b; (2e) product of the third pathway, 2c. Bond distances are in angström, and bond angles in degrees. CAS-MCSCF/6-31G(d) (bold) and MP2/6-31G(d) values are shown.

way by way of a series of constrained optimizations carried out at different P–H distances. This allowed to assess a barrier height of ~ 69 kcal mol^{-1} (reported in Fig. 5 as a bracketed value). All energy differences, as determined at the CAS-MCSCF level, result to be rather close to those subsequently computed at the (single-reference) MP2 level (Table III).

Very moderate depressions in the energy hypersurface, separating most transition structures from the relevant dissociation limits, correspond to loose associations of the two resulting moieties (geometries not reported). The importance of these complexes appears to be quite dubious. Figure 5 (right-hand side) summarizes the features of the H migration and H atom dissociations just discussed.

For the two more viable pathways the energy plateau corresponding to the two separated moieties $P^+=PH_2$ (doublet) and H is located at an energy value definitely close to those of the two transition structures; therefore, the overall features of the dissociation curves are evidently dictated by the thermochemistry, given that a barely significant overhead is detected for the inverse process.

Examining in more detail the CAS-MCSCF results, it can be observed that the large coefficient of the dominant configuration is significantly lowered in the two transition structures 2a and 2b, with respect to its value for the structures shown in Fig. 3. These are, perhaps not fortuitously, the CAS-MCSCF structures for which the MP2 results are to some extent at variance; 2a, as mentioned above, could not be located and might not exist on the MP2 surface; 2b presents significant differences between the two values of the P—H distance and HPP angle.

5. H_2 *dissociations from* $P–PH_3^+$ *and* $HP^+–PH_2$ *(pathways 3)*

This process can take place either from 1a or, as an alternative, from 1c. Both fragmentations occur with complete loss of the ternary symmetry of the initial adduct. The C_1 transition structure, relevant to the first pathway (Fig. 6, 3a), has an energy comparable with those of the two preceding dissociation transition structures (Table II). Also the corresponding dissociation limit ($P=P^+-H$ and H_2, Fig. 6, 3c) is rather close to the previous one, although slightly lower in energy (Table II). The multideterminantal wave function for this dissociation limit presents some non-negligible contribution from singly and doubly excited configurations (compare Table II, rightmost column). Thus, this is perhaps the critical point for which the single-reference MP2 energy value is more questionable.

Analysis of the MCSCF wave function allows us to trace back the reason of the lowered symmetry of 3a or 3b to the different symmetry of the ground triplet states in the reactant and product molecules, 1a vs 3a or 1c vs 3b. In the case of a model dissociation with enforced C_s symmetry the presence of a real crossing between two electronic states is observed, as shown in Fig. 7, for the 1a–3c pathway. The ground state in 1a is antisymmetric (A) (as is the case for 1c), while in 3c it is symmetric (S). In fact, one of the two unpaired elec-

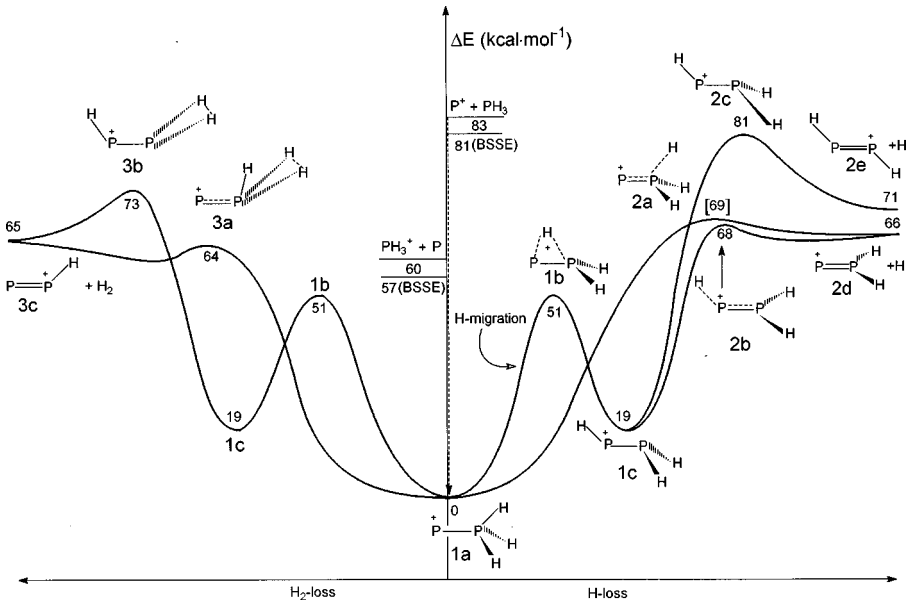

FIG. 5. MP2/6-31G(d) energy profiles (energy values are reported as integers). (Right) H atom migration pathway from 1a and H atom dissociation pathways from 1a and 1c. The bracketed value is obtained from a series of constrained optimizations carried out at fixed P–H distances. (Left) H atom migration pathway from 1a and H_2 molecule dissociation from 1a and 1c.

trons lies (in both 1a and 1c) in a $p\pi$ orbital which is orthogonal to the PPH plane. On the other hand, the two unpaired electrons left on the triplet $P{=}PH^+$ moiety are located in two in-plane π-type orbitals (one in phase, the other out of phase) to which the 1s orbital of the remaining hydrogen participates to a moderate extent. The reaction is thus allowed to take place in correspondence of an avoided crossing only if the symmetry lowering to C_1 permits the two states to mix.

The 1c–3c pathway, i.e., the H_2 detachment from $HP^+–PH_2$, requires overcoming a higher energy barrier than the 1a–3c.

Figure 5 (left-hand side) provides an overall picture of the features just discussed (H_2 detachment processes are shown on the left).

6. QCISD energy differences

A further assessment of the energetics of the H or H_2 dissociation processes was then accomplished by quadratic configuration interaction single-point energy calculations, carried out at the QCISD(T)/6-311G(2d,2p) level. The MP2/6-31G(d) geometries, obtained for a series of frozen P–H distance values by constrained energy minimizations, were used. Approximate QCI energy profiles for the 1a–2d and 1c–2d dissociations were thus obtained. These two profiles are simpler than those discussed above (compare Fig. 5), because both transition structures (maxima) and complexes (local minima) seem to disappear, leaving just an uphill pathway, departing from each minimum, whose slope attenuates and smoothly merges into the dissociation limit. Unfortunately, incomplete profiles were obtained for the other processes, because of convergence problems. For this reason, only the reaction energies have been collected in Table IV. These values appear to be in reasonable agreement with those obtained at the two lower computational levels.

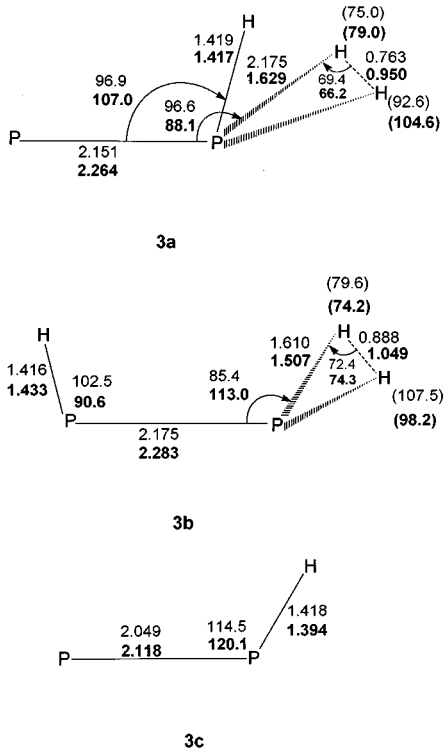

FIG. 6. H_2 molecule dissociation from $P–PH_3^+$ and $HP^+–PH_2$; (3a) transition structure for the dissociation from 1a; (3b) transition structure for the dissociation from 1c; (3c) product. Bond distances are in angström, and bond angles in degrees. CAS-MCSCF/6-31G(d) (bold) and MP2/6-31G(d) values are shown.

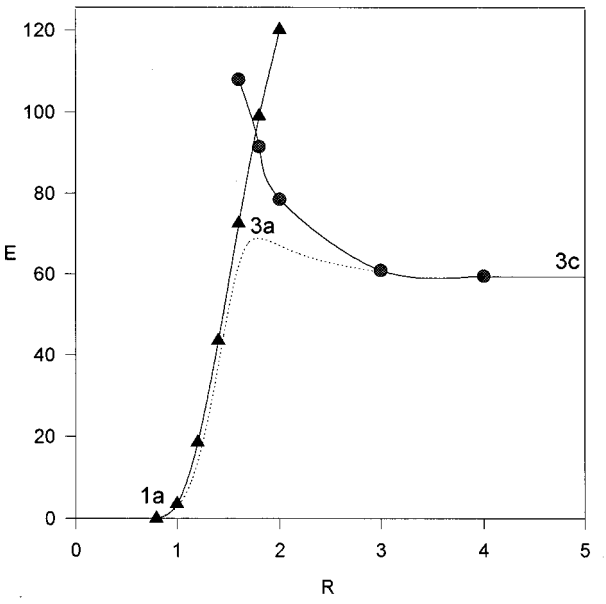

FIG. 7. Energy profiles relevant to the real crossing between two electronic states, in a model dissociation with enforced C_s symmetry; antisymmetric ground state of 1a (▲); symmetric ground state of 3c (●); avoided crossing (dashed line), found if the C_s constraint is removed. R is the distance between the P atom and the midpoint of the H–H bond in H_2 which is leaving.

7. Thermochemistry

Formation enthalpies for the five cations considered in this paper have been calculated in two different ways, and are reported in Table V.

The first estimate (Method A, columns 1 and 2) relies on tabulated experimental formation enthalpies.[31] These, combined with the computed standard reaction enthalpy relevant to the formation of a particular ion, provide an estimate of its $\Delta H_f^0(P_2H_n^+)$. In the first column of Table V, MP2/ 6-31G(d), the vibrational frequencies, used to compute the thermal correction necessary to obtain $\Delta H_f^0(P_2H_n^+)$, have been scaled as suggested in Ref. 36. In the second column the values reported have been obtained by using unscaled MP2/6-31G(d) frequencies. The differences appear to be unsignificant, because the largest change is 0.3 kcal mol^{-1}. Decimal figures are reported just to allow appreciation of the extent to which scaling of the frequencies affects the computed data. Actually, all computed data reported in Table V have no significant decimal figures, because $\Delta H_f^0(P^+)$ is reported in Ref. 31 without any.

The second estimate (Method B, columns 3 and 4) more heavily relies on computed data; it has been obtained by the method proposed by Pople *et al.*[37] The procedure is outlined in Scheme 2.

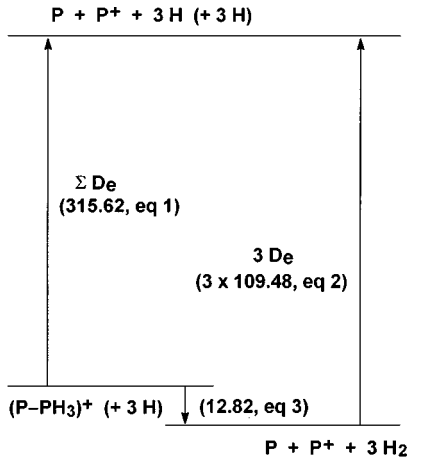

$$(P\text{–}PH_3)^+ \longrightarrow P + P^+ + 3H \quad (1)$$

$$H_2 \longrightarrow 2H \quad (2)$$

$$(P\text{–}PH_3)^+ + 3H \longrightarrow P + P^+ + 3H_2 \quad (3)$$

ΣD_e is the required atomization energy [Eq. (1)] to be used in the estimate of ΔH_f^0. This is obtained as a difference between the ΔE of the known atomization energy of H_2 [Eq. (2)] and the isogyric reaction [Eq. (3)]. The method was used with the following modifications: (i) the QCISD(T)/ 6–311G($2d$,$2p$) energies (reported in Table IV) have been directly used throughout to evaluate the energy difference relevant to the isogyric Eq. (3); (ii) instead of the ZPE correction to the energy, the full thermal correction has been applied (as outlined in Ref. 36). Again, two columns report data obtained by using scaled and unscaled frequencies. Also using method B, the variation between the two sets of values is at most by 1 kcal mol^{-1}.

Differences between the results of the two methods (A and B) are within 9 kcal mol^{-1} and this is not surprising as the methods are substantially different. In fact, although both are hybrid methods which combine experimental and computational data, they differ in two aspects; (i) method B is based on experimental enthalpies of formation of atoms only, whilst method A makes use also of molecular formation enthalpies; (ii) method A directly uses the computed reaction energies of Table IV, whilst method B more carefully exploits the energy of an isogyric reaction.

The enthalpies of formation of the $P_2H_n^+$ ions have been previously obtained by experimental methods[21] and are shown in column 5 for comparative purposes. A general reasonable agreement is observed between both theoretical re-

TABLE V. Heats of formation of the $P_2H_n^+$ ions (kcal mol^{-1}).

	ΔH_f°				
Ion	Method A[a] scaled	Method A[a] unscaled	Method B[b] scaled	Method B[b] unscaled	Experimental[c]
$P_2H_3^+$	241.2	241.3	245.9	246.9	234
$HP_2H_2^+$	254.9	254.9	262.1	263.0	234
$P_2H_2^+$	252.7	252.4	259.8	260.4	261
HP_2H^+	262.5	262.4	270.0	270.8	261
P_2H^+	298.0	297.8	305.3	305.6	289

[a]Calculated from theoretical enthalpies of reaction (from Table IV) and experimental enthalpies of formation (Ref. 31); scaled as suggested in Ref. 36.
[b]Calculated on data computed as in Ref. 37; scaled as suggested in Ref. 36.
[c]Fehlenr and Callen (Ref. 21).

sults and experimental data, the percentage error staying within 6% in most cases. The only exception is the $HP_2H_2^+$ ion, the less stable isomeric form of the $P_2H_3^+$ species, which gives a maximum difference of 12% between 263.0 kcal mol^{-1} (column 4) and 234 kcal mol^{-1} (column 5). In general, the highest discrepancies are observed for the $HP_2H_2^+$ and HP_2H^+ ions, which are less stable than their isomers and, therefore, are expected to contribute at a lower extent to the species whose enthalpies of formation are measured in experimental studies.

Finally, the enthalpy of the charge-exchange reaction shown in Table IV (-15.2 kcal mol^{-1}) is very similar to that calculated on the basis of the formation enthalpies reported in the literature (-13.7 kcal mol^{-1}).[31]

V. CONCLUSIONS

Hydrogen atom and hydrogen molecule dissociations from the initial adduct $P–PH_3^+$, produced by collision of triplet P^+ onto phoshine, as well as from the rearranged ion $HP^+–PH_2$, have been investigated by correlated *ab initio* methods. The potential energy released in the adduct formation is estimated to be 78–79 kcal mol^{-1}, and sets a reference value for judging the feasability of subsequent rearrangement and cleavage processes. The former, connecting the two mentioned ions, is found to be very easy (requiring $\sim$50 kcal mol^{-1}). The H atom dissociations present two viable pathways (one from $P–PH_3^+$, the other from $HP^+–PH_2$), each required to overcome a barrier of less than 70 kcal mol^{-1}, and leading to H and $P^+=PH_2$ fragments. In contrast, a third pathway, leading to a different dissociation limit (HP=PH+H), appears to be less easily followed, given that the related energy barrier is very close to the mentioned reference energy value. Two hydrogen molecule dissociation processes have also be considered, originating again either from $P–PH_3^+$ or from $HP^+–PH_2$. The former presents a barrier just slightly lower than the two lower ones for H dissociation (64 kcal mol^{-1}). The latter originates from the rearranged adduct but leads to the same dissociation limit; it presents a higher energy pathway, which, although lower than the reference energy value, appears to be less viable. The energy differences among the three more probable fragmentation processes are too small to allow a quantitative prediction of the preferences exhibited by this reacting system. On the other hand, the largest kinetic constant ratio obtained from the experiments for reactions of P^+ with PH_3 is $\sim$12 (Table I), and thus appears to be in fairly good agreement with the description provided by the theoretical calculations. Moreover, the rate constants determined experimentally indicate that clustering reactions in phosphine starting from P^+ proceed quite slowly and only an ion species containing up to three phosphorus atoms is observed, while the reactions occurring with the highest rate constants generally lead to the formation of the unreactive phosphonium ion, PH_4^+.

Finally, the enthalpies of formation of the $P_2H_n^+$ ions calculated theoretically show a reasonable agreement with those previously determined by experimental methods.

ACKNOWLEDGMENT

The authors thank MURST for financial support.

[1] Y. Maruyama, T. Inabe, L. He, T. Terui, and K. Oshima, Bull. Chem. Soc. Jpn. **64**, 811 (1991).
[2] D. Briand, M. Sarret, F. Le Bihan, O. Bonnaud, and L. Pichon, Mater. Sci. Technol. **11**, 1207 (1996).
[3] G. Ritter, B. Tillack, and D. Knoll, Mater. Res. Soc. Symp. Proc. **387**, 341 (1995).
[4] C. Li, S. John, E. Quinones, and S. Banerjee, J. Vac. Sci. Technol. A **14**, 170 (1996).
[5] R. W. Collins, J. S. Burnham, S. Kim, J. Koh, Y. Lu, and C. R. Wronski, J. Non-Cryst. Solids **198**, 981 (1996).
[6] J. Simon, R. Feurer, A. Reyner, and R. Morancho, J. Anal. Appl. Pyrolysis **26**, 27 (1993).
[7] A. M. Hodge, A. G. Morpeth, and P. C. Stevens, in *Fine Chemicals for the Electronic Industry II*, edited by D. J. Ando and M. G. Pellat (The Royal Society of Chemistry, London, 1991), Special Publication No. 88.
[8] P. Antoniotti, P. Benzi, M. Castiglioni, L. Operti, and P. Volpe, Chem. Mater. **4**, 717 (1992).
[9] P. Antoniotti, P. Benzi, M. Castiglioni, L. Operti, and P. Volpe, Radiat. Phys. Chem. **48**, 457 (1996).
[10] P. Benzi, L. Operti, G. A. Vaglio, P. Volpe, M. Speranza, and R. Gabrielli, J. Organomet. Chem. **354**, 39 (1988); **373**, 289 (1989); Int. J. Mass Spectrom. Ion Processes **100**, 647 (1990); L. Operti, M. Splendore, G. A. Vaglio, P. Volpe, M. Speranza, and G. Occhiucci, J. Organomet. Chem. **433**, 35 (1992); L. Operti, M. Splendore, G. A. Vaglio, and P. Volpe, Spectrochim. Acta **49A**, 1213 (1993); Organometall. **12**, 4509 (1993); **12**, 4516 (1993); L. Operti, M. Splendore, G. A. Vaglio, A. M. Franklin, and J. F. J. Todd, Int. J. Mass Spectrom. Ion Processes **136**, 25 (1994); J. F. Gal, R. Grover, P. C. Maria, L. Operti, R. Rabezzana, G. A. Vaglio, and P. Volpe, J. Phys. Chem. **98**, 11 978 (1994); P. Benzi, L. Operti, R. Rabezzana, M. Splendore, and P. Volpe, Int. J. Mass Spectrom. Ion Processes **152**, 61 (1996).
[11] S. Wlodek and D. K. Bohme, J. Am. Chem. Soc. **110**, 2396 (1988).
[12] I. Haller, J. Phys. Chem. **94**, 4135 (1990).
[13] L. Operti, R. Rabezzana, G. A. Vaglio, and P. Volpe, J. Organomet. Chem. **509**, 151 (1996).
[14] M. L. Mandich, W. D. Reents, Jr., and M. F. Jarrold, J. Chem. Phys. **88**, 1703 (1988); M. L. Mandich, W. D. Reents, Jr., and K. D. Kolenbrander, *ibid*. **92**, 437 (1990); M. L. Mandich and W. D. Reents, Jr., *ibid*. **95**, 7360 (1991); W. D. Reents, Jr. and M. L. Mandich, *ibid*. **96**, 4429 (1992).
[15] P. Antoniotti, L. Operti, R. Rabezzana, G. A. Vaglio, P. Volpe, J. F. Gal, R. Grover, and P. C. Maria, J. Phys. Chem. **100**, 155 (1996).
[16] J. Berkowitz, L. A. Curtiss, S. T. Gibson, J. P. Greene, G. L. Hillhouse, and J. A. Pople, J. Chem. Phys. **84**, 375 (1986).
[17] K. Raghavachari, J. Chem. Phys. **88**, 1688 (1988); **92**, 452 (1990); **95**, 7373 (1991); **96**, 4440 (1992).
[18] J. M. H. Pakarinen, P. Vainiotalo, C. L. Stumpf, D. T. Leeck, P. K. Chou, and H. I. Kenttämaa, J. Am. Soc. Mass Spectrom. **7**, 482 (1996).
[19] A. Largo, J. R. Flores, C. Barrientos, and J. M. Ugalde, J. Phys. Chem. **95**, 170 (1991); E. Del Rio, C. Barrientos, and A. Largo, *ibid*. **96**, 6607 (1993); **100**, 14 643 (1996); M. Esseffar, A. Luna, O. Mó, and M. Yáñez, Chem. Phys. Lett. **209**, 557 (1993).
[20] M. T. Bowers, in *Gas Phase Ion Chemistry* (Academic, New York, 1979), Vol. 1.
[21] T. P. Fehlner and R. B. Callen, Adv. Chem. Ser. **72**, 181 (1968); D. Holtz, J. L. Beauchamp, and J. R. Eyler, J. Am. Chem. Soc. **92**, 7045 (1970).
[22] M. Decouzon, J. F. Gal, P. C. Maria, and A. S. Tchinianga (personal communication).
[23] H. B. Schlegel, in *Computational Theoretical Organic Chemistry*, edited by I. G. Csizsmadia and R. Daudel (Reidel, Dordrecht, 1981), p. 129; H. B. Schlegel, J. Chem. Phys. **77**, 3676 (1982); H. B. Schlegel, J. S. Binkley, and J. A. Pople, *ibid*. **80**, 1976 (1984); H. B. Schlegel, J. Comput. Chem. **3**, 214 (1982).
[24] M. A. Robb and R. H. A. Eade, NATO Adv. Study Inst. Ser. C **67**, 21 (1981).
[25] C. Møller and M. S. Plesset, Phys. Rev. **46**, 618 (1934); J. S. Binkley and J. A. Pople, Int. J. Quantum Chem. **9**, 229 (1975). The computations were carried out without the ''frozen core'' approximation.
[26] R. Ditchfield, W. J. Hehre, and J. A. Pople, J. Chem. Phys. **56**, 2252

(1972); P. C. Hariharan, and J. A. Pople, Theor. Chim. Acta **28**, 213 (1973); M. M. Francl, W. J. Pietro, W. J. Here, J. S. Binkley, M. S. Gordon, D. J. Defrees, and J. A. Pople, J. Chem. Phys. **77**, 3654 (1982); K. Raghavachari, J. S. Binkley, R. Seeger, and J. A. Pople, *ibid*. **72**, 650 (1980); A. D. McLean and G. S. Chandler, *ibid*. **72**, 5639 (1980).

[27] J. A. Pople, A. P. Scott, M. W. Wong, and L. Radom, Isr. J. Chem. **33**, 345 (1993).

[28] J. A. Pople, M. Head-Gordon, and K. Raghavachari, J. Chem. Phys. **87**, 5968 (1987).

[29] See, for instance, W. J. Hehre, L. Radom, P.v.R Schleyer, and J.A Pople, in *Ab Initio Molecular Orbital Theory* (Wiley, New York, 1985); S. M. Bachrach and A. Streitwieser Jr., J. Am. Chem. Soc. **106**, 2283 (1984); see also the discussion, in J. H. van Lenthe, C. C. M. van Duijneveldt-van de Rijdt, and F. B. van Duijneveldt, *Ab Initio Methods in Quantum Chemistry II*, edited by K. P. Lawley (Wiley, New York, 1987), p. 521, and references therein.

[30] M. J. Frisch, G. W. Trucks, H. B. Schlegel, P. M. W. Gill, B. G. Johnson, M. A. Robb, J. R. Cheeseman, T. Keith, G. A. Petersson, J. A. Montgomery, K. Raghavachari, M. A. Al-Laham, V. G. Zakrzewski, J. V. Ortiz, J. B. Foresman, J. Cioslowski, B. B. Stefanov, A. Nanayakkara, M. Challacombe, C. Y. Peng, P. Y. Ayala, W. Chen, M. W. Wong, J. L. Andres, E. S. Replogle, R. Gomperts, R. L. Martin, D. J. Fox, J. S. Binkley, D. J. Defrees, J. Baker, J. P. Stewart, M. Head-Gordon, C. Gonzalez, and J. A. Pople, Gaussian Inc., Pittsburgh, Pennsylvania, 1995.

[31] S. G. Lias, J. E. Bartmess, J. F. Liebman, J. L. Holmes, R. D. Levin, and W. G. Mallard, J. Phys. Chem. Ref. Data Suppl. **17** (1988).

[32] F. Y. Yu, T. M. H. Cheng, V. Kempter, and F. W. Lampe, J. Phys. Chem. **76**, 3321 (1972).

[33] The eight active orbitals chosen are the two mentioned P–PH_3^+ p orbitals localized on the P atom carrying no hydrogens, which are perpendicular to the P–P bond, plus the σ, π, and π' of the PH_3 group, as well as their antibonding counterparts, σ^*, π^*, and π'^*. In this space a full CI is performed (2352 configurations) and the molecular orbitals are allowed to relax. When some nuclear rearrangement occurs, these starting orbitals mix consistently to provide other combinations, which are discussed in the following subsections as necessary.

[34] L. Mahé and J. C. Barthelat, J. Phys. Chem. **99**, 6819 (1995). Compare Ref. 19(b) in which a different result was found for the P–$^+NH_3$ adduct; the 1.91 Å P–N bond and the positive value of the Laplacian in the P–N region lead to the conclusion that P^+ and NH_3 are held together in an electrostatic complex.

[35] H. B. Schlegel, J. Chem. Phys. **84**, 4530 (1986).

[36] J. B. Foresman and Æ. Frisch, in *Exploring Chemistry with Electronic Structure Methods* (Gaussian, Pittsburgh, 1996), p. 64.

[37] J. A. Pople, B. T. Luke, M. J. Frisch, and J. S. Binkley, J. Phys. Chem. **89**, 2198 (1985).